EXTERIOR ORIENTATION DETERMINATION OF MOMS-02 THREE-LINE IMAGERY: EXPERIENCES WITH THE AUSTRALIAN TESTFIELD DATA

Clive Fraser and Juliang Shao

Department of Geomatics
The University of Melbourne
Parkville, Victoria 3052, Australia
Email: Clive_Fraser@mac.unimelb.edu.au
jsha@sunrise.sli.unimelb.edu.au

Commission III, Working Group 1

KEY WORDS: Three-Line Satellite Imagery, Triangulation, Accuracy

ABSTRACT

The three-line imagery recorded by MOMS-02 on its inaugural mission in 1993 has provided an opportunity to evaluate the photogrammetric potential of such satellite imaging systems. Among the areas covered by MOMS-02/D2 three-fold stereo imagery was a 110 km x 40 km swath in Central Australia which has been selected as an accuracy testbed for ground point determination and DTM extraction. This paper first discusses the establishment of the Australian Testfield, both in respect to photogrammetric requirements and the collection of ground truth data by GPS survey. The triangulation accuracy of MOMS-02/D2 imagery is then considered. A review of the mathematical model is provided and the results of a series of bundle adjustments employing different control point configurations, numbers of orientation images and orders of interpolation functions are analysed. The findings of the accuracy evaluation are discussed and compared to theoretical expectations.

1. INTRODUCTION

With the launch in April 1993 of the Modular Opto-electronic Multispectral Stereo Scanner, MOMS-02, as part of the German Spacelab Mission D2 on board the Space Shuttle, the photogrammetric community was presented with a first opportunity to evaluate the metric potential of a space-borne high-resolution three-line imaging system. MOMS-02 was specifically designed to generate digital topographic mapping data, primarily through automated DTM extraction to accuracies of about 5m, and through the generation of digital orthoimagery with adequate resolution and geometric accuracy to meet map specifications at 1:50,000 scale and larger (e.g. Ackermann et al, 1990; Seige, 1993; Fritsch, 1994).

Simulation studies (Ebner et al, 1992) had indicated that object point triangulation accuracies to better than 5m in planimetry and up to 5m in height should be possible from the along-track, three-fold coverage of MOMS-02. Imagery obtained from the D2 mission would provide verification or otherwise of predictions of this metric performance level.

One of the Mode 1 panchromatic imaging sequences recorded during the 10-day D2 mission, namely scene 17 of Orbit 75b, covered a swath of 110km x 40km in the north eastern region of Central Australia. Through a collaborative arrangement between the Department of Geomatics at The University of Melbourne and MOMS-02 photogrammetric research teams in Germany, this area was chosen as an 'accuracy testbed' for exterior orientation determination and ground point triangulation. The main requirement for the 'Australian Testfield' was the provision of a well distributed array of image-identifiable ground control points which would facilitate a comprehensive metric evaluation of MOMS-02/D2 three-fold stereo imagery.

The purpose of this paper is to report on two facets of the overall investigation into the cartographic potential of MOMS-02, namely the establishment of the GPS-surveyed accuracy testbed and the investigation into ground point triangulation accuracy attainable with this high-resolution (HR) imaging system.

2. THE AUSTRALIAN TESTFIELD

The testfield covered mostly flat and featureless terrain which displayed an elevation range of only 70m. One of the primary requirements for the MOMS-02 image testbed was the availability of image-identifiable ground control points which could be accurately surveyed by GPS. In this regard the testfield left a little to be desired. Image identifiable points were effectively restricted to the dams and track/fence intersections of the Lake Nash cattle station. To achieve triangulation accuracies at the 5-10m level, sub-pixel image mensuration precision is required. This in turn is

contingent upon the provision of clear, unambiguous targets in the imagery. Only one category of target was found which adequately fulfilled these requirements, this being the water surface area of dams. Even these targets were somewhat deficient in that most dams had changing water levels and diameters of 30m or less, which translates to only a 2-3 pixel width in the off-nadir imagery. Moreover, there was an insufficient number of such targets.

A second category of targets, which were clearly visible in the imagery, were dam embankments. Whereas, the centroid of an embankment image was usually clear, great difficulty was encountered in finding the corresponding position on the ground. Errors of a pixel or more could be expected in this target point correspondence operation and it was not always feasible to assess which were 'poor' targets. A last general category of targets comprised road (few), track and fence intersections, or more correctly in the latter case, intersections of graded tracks along fencelines. In most cases these presented reasonable image targets, but there was the complication that the imagery was acquired in 1993, with the ground survey being carried out in 1994 and 1995. In each dry season a program of grading occurs in which roads, tracks and fencelines are re-graded following wet-season damage, not necessarily in exactly the same location as in the previous year.

Notwithstanding identification problems, about 80 well distributed image-identifiable ground control points were established. Two GPS campaigns were mounted to provide the necessary ground truth data. The GPS survey technique employed two base stations and roving receivers, with an occupation time of 30 minutes at each point. Processing of the data from the 122 baselines observed indicated that a positional accuracy (relative) of 10cm had been achieved.

To help alleviate some of the problems with point identification a number of the stations were re-occupied in the 1995 field campaign. Re-observation of these points confirmed the quality estimates for the GPS survey. A last phase of the second campaign was the survey of a 16km 3-D profile along an image-identifiable fenceline via kinematic GPS. This heighting profile was established to facilitate an evaluation of the precision of MOMS-02 DTM extraction. Further details of the GPS survey phase are provided in Fraser et al (1996).

The last component in the establishment of the Australian testfield comprised the image mensuration stage. Multiple image coordinate measurements were observed for each of the GPS-surveyed ground points. In addition to the set of observations made in monoscopic mode on an Intergraph ImageStation digital photogrammetric workstation at The University of Melbourne, independent measurements with varying levels of image enhancement were also made by MOMS-02 research groups in Germany and Switzerland.

Following qualitative analysis, backed up by the results of a process of 2-D image-to-ground transformation, a subset of 56 3-ray points and an additional six 2-ray points were deemed likely to display measurement accuracies at the 1-pixel (10μm) level or better. The distribution of these points is shown in Figure 1. Some 40 of the image points were estimated to display a standard error of better than 0.5 pixel in all three imaging channels, based primarily on image quality. In this paper we consider two such data sets, one from Melbourne (three channels) and one from Dr E. Baltsavias of ETH Zurich (forward and aft channels only). In the context of the target identification problems referred to it is noteworthy that the RMS discrepancy between these two independently observed data sets was 0.7 pixels or 7μm, which is a little higher than desired.

3. MATHEMATICAL MODEL

The functional model adopted for the exterior orientation/triangulation is a form of the photogrammetric bundle adjustment adapted to accommodate the geometric conditions of three-line imagery (Ebner et al, 1992):

$$x = x_0 - f\frac{R_{11}(X-X_0)+R_{21}(Y-Y_0)+R_{31}(Z-Z_0)-\left[M_{11}\Delta X+M_{21}\Delta Y+M_{31}\Delta Z\right]}{R_{13}(X-X_0)+R_{23}(Y-Y_0)+R_{33}(Z-Z_0)-\left[M_{13}\Delta X+M_{23}\Delta Y+M_{33}\Delta Z\right]}$$

$$y = y_0 - f\frac{R_{12}(X-X_0)+R_{22}(Y-Y_0)+R_{32}(Z-Z_0)-\left[M_{12}\Delta X+M_{22}\Delta Y+M_{32}\Delta Z\right]}{R_{13}(X-X_0)+R_{23}(Y-Y_0)+R_{33}(Z-Z_0)-\left[M_{13}\Delta X+M_{23}\Delta Y+M_{33}\Delta Z\right]} \quad (1)$$

Equation 1 expresses the image coordinate observations x,y as a function of the following parameters: the elements of interior orientation x_o, y_o and f; the coordinates X, Y, and Z of the object point; the exterior orientation elements X_o, Y_o, Z_o, ω_o, φ_o, and κ_o of the HR, nadir-looking lens; and the relative positional and orientation elements ΔX, ΔY, ΔZ, $\Delta\omega$, $\Delta\varphi$, and $\Delta\kappa$ of the off-nadir sensor line with respect to the projection centre of the HR lens. The rotation matrix R is obtained as the product of rotation matrices $M(\Delta\omega, \Delta\varphi, \Delta\kappa)$ and $D(\omega_o, \varphi_o, \kappa_o)$.

In the standard along-track stereo imaging mode, without cross strips, self-calibration is not possible and thus a number of the parameters forming the

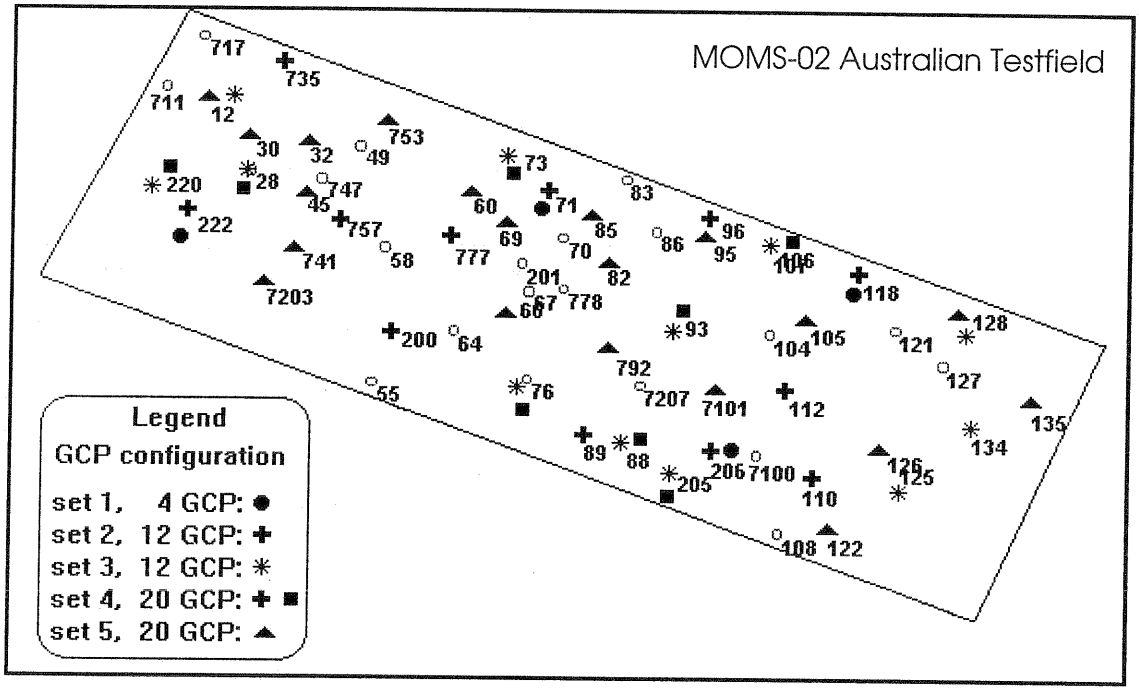

Figure 1: Control point distribution

extended collinearity equation must be determined via camera calibration. These include the interior orientation elements and the parameters $\Delta\omega$, $\Delta\varphi$, $\Delta\kappa$, ΔX, ΔY and ΔZ for the forward- and backward-looking channels. For the processing of the MOMS-02/D2 data, the inclination angle of $\Delta\varphi = \pm 21.457^\circ$ was the only parameter of these six to have a non-zero value.

In order to achieve a solution for the collinearity equations at each scan line, a re-parameterization of the exterior orientation elements by time dependent polynomial functions is adopted. Quadratic functions have been used for stereo restitution of both SPOT (Kratky, 1989) and MOMS-02/D2 imagery (Dorrer et al, 1995), whereas for the triangulation of MOMS-02 three-line imagery Lagrange polynomials of third order have been proposed (Ebner et al, 1992; Kornus et al, 1995). Under the latter approach, which has been adopted in this investigation, exterior orientation elements are recovered for so-called orientation images (OIs) at given scan-line intervals. The Lagrange polynomials then model the assumed smooth variation of sensor position and attitude over each interval of m scan lines between adjacent OIs. For a third-order curve the model is given as:

$$P_3(t) = \sum_{i=OI-1}^{OI+2} P(t_i) \prod_{\substack{j=OI-1 \\ j\neq i}}^{OI+2} \frac{t-t_j}{t_i-t_j} \qquad (2)$$

where $P_3(t)$ at time t is a linear combination of $P(t_i)$ at the four neighbouring OIs.

One of the perceived advantages of the Lagrange polynomial approach is that the interpolation is dependent upon only the nearest one or two OIs on each side of a given scan line for first- to third-order interpolation. Thus, for a third-order approximation, four OIs are employed, whereas for a first-order model the interpolation would be linear between two OIs. One of the aims of the present work was to investigate the impact of the order of the function on triangulation accuracy.

For the bundle adjustment of the MOMS-02/D2 imagery, the following observation equation set was employed:

$$\begin{aligned}
v &= At + Bx - l; \quad P_l \\
v_t &= t + C_0 t_a + C t_b - l_t; \quad P_t \\
v_x &= x - l_x; \quad P_x \\
v_{ta} &= t_a - l_{ta}; \quad P_{ta} \\
v_{tb} &= t_b - l_{tb}; \quad P_{tb}
\end{aligned} \qquad (3)$$

where A indicates the coefficient matrix of the unknown exterior orientation parameters t; B is the coefficient matrix of the ground coordinate vector x; t_a and t_b are the vectors of shift and drift terms whose coefficient matrices are given by C_0 and C; v_i, l_i and P_i are residual and discrepancy vectors, and weight matrices, respectively. The weight matrices P_x, P_{ta} and P_{tb} are primarily employed to allow the associated

parameters to be carried as fixed or free unknowns. The shift and drift parameters are employed to model biases in the exterior orientation parameters t in instances where absolute constraints are imposed (via P_t) through the provision of prior estimates for the position and attitude of the sensor.

A standard fold-in solution approach involving an elimination of the object point coordinates x is employed in the solution of the least-squares normal equation system generated from Eqs. 3. The unknown orientation elements t are first obtained as follows:

$$t = [S + P_t - (P_t C_0 \quad P_t C) Q \begin{pmatrix} C_0^T P_t \\ C^T P_t \end{pmatrix}]^{-1} L \qquad (4)$$

where

$$L = [\overline{C} + P_t l_t - (P_t C_0 \quad P_t C) Q \begin{pmatrix} C_0^T P_t l_t + P_{ta} l_{ta} \\ C^T P_t l_t + P_{tb} l_{tb} \end{pmatrix}]$$

$$Q = \begin{pmatrix} C_0^T P_t C_0 + P_{ta} & C_0^T P_t C \\ C^T P_t C_0 & C^T P_t C + P_{tb} \end{pmatrix}^{-1}$$

$$\overline{B} = (B^T P_l B + P_x)_j^{-1}$$

$$S = \sum_1^n S_j, \quad S_j = (A^T P_l A)_j - (A^T P_l B)_j \overline{B} (B^T P_l A)_j$$

$$\overline{C} = \sum_1^n \overline{C}_j, \quad \overline{C}_j = (A^T P_l l)_j - (A^T P_l B)_j \overline{B} (B^T P_l l + P_x l_x)_j$$

With 3 x 3 back substitution the solution for the XYZ coordinates of each ground point j is obtained as

$$x_j = \overline{B}[(B^T P_l l + P_x l_x)_j - (B^T P_l A)_j t] \quad j = 1,2,\cdots n. \qquad (5)$$

with the associated covariance matrix being determined by the expression

$$C_{x_j} = \overline{B} + \overline{B}(B^T P_l A)_j C_t (A^T P_l B)_j \overline{B}] \quad j = 1,2,\cdots n. \qquad (6)$$

Finally, the systematic error terms t_a and t_b are determined, if included. In their analysis of MOMS-02/D2 ground point determination, Kornus et al (1995) identified a significant timing offset between the Space Shuttle navigation data and the image recording times. This amounted to 0.48 seconds or several kilometres. In recognition of uncertainties regarding the quality of the navigation data, an examination of the effectiveness of imposing exterior orientation constraints coupled with shift and drift parameters was not thoroughly pursued for the present investigation. In the few bundle adjustments conducted which included *a priori* weights P_t and the parameters t_a and t_b, it was concluded that the shift and drift terms had little impact on accuracy for the Australian Testfield data.

4. INSIGHTS FROM 2-D TRANSFORMATION

From the standpoint of evaluating the accuracy of DTM extraction, the flat terrain of the Australian Testfield was a disadvantage. From a ground point determination perspective, however, it was advantageous in one respect, namely that 2-D image-to-ground transformation had the potential of providing an insight into the quality of the photogrammetric data. A series of affine, and second- and third-order polynomial transformations were made between the GPS ground control and the measured image coordinates (Melbourne set) in each of the three channels. The aim of this exercise was to reveal gross errors in the image mensuration stage and to provide an indication of the appropriate order to be adopted for the Lagrange polynomials.

Transformations covering the full 110 km long testfield were first carried out, and this was followed by a second stage which considered 2-D transformations in four 'localised' areas, each of approximately 25 km in length. The resulting RMS values of XY ground point residuals from the transformations are listed in Table 1. In the table it can be seen that, as expected, localised transformations yielded smaller residuals than those for the full testfield, except at the eastern end of the area (Set 4) which was a region of poorer control point quality. The following points regarding the results in Table 1 are noteworthy in the context of this investigation:

- There is essentially no distinction between the results for the 4.5m HR and 13.5m lower-resolution (LR) channels. This may be attributable to either poor ground control point identification or the lower quality of the nadir-looking imagery.
- There is generally a notable improvement in the second-order transformation as compared to the first-order model, but a more modest improvement when proceeding from a second-order to a third-order model, especially in the smaller areas (Sets 1-4). The implication here is that a Lagrange polynomial of second- or third-order might be most appropriate for the subsequent interpolation of exterior orientation parameters in the bundle adjustment.
- The second- and third-order models yield a planimetric ground point accuracy at the 9m level (0.7 pixels in the LR imagery) over the full 110

Table 1: RMS values of residuals from 2-D transformations between image coordinates and ground control point planimetric coordinates for both the entire testfield and four 25 km x 40 km sections, each containing about 20 points. Results are given for each channel, for first-, second- and third-order models. Units are metres.

CHANNEL	FULL TESTFIELD			SET 1			SET 2			SET 3			SET 4		
	1st	2nd	3rd	1st	2nd	3rd	1st	2nd	3rd	1st	2nd	3rd	1st	2nd	3rd
5, nadir	12.9	9.7	9.4	9.3	8.3	6.1	9.4	6.7	5.1	11.1	5.8	4.9	10.1	9.5	9.1
6, forward	11.4	8.7	8.7	9.0	8.6	6.1	8.6	6.0	5.0	10.0	6.0	5.0	11.9	11.2	10.8
7, backward	12.4	9.1	8.7	10.3	9.1	6.9	10.1	8.1	6.8	10.6	7.5	6.6	11.8	11.0	9.8

km length of the testfield, and at the 5-7m level (0.4-0.5 pixels) in three of the four 1000 km^2 areas. While these values are impressive in their own right, what is more important is the inference that the bundle adjustment should yield a similar or better planimetric triangulation accuracy.

5. TRIANGULATION RESULTS

5.1 Overview

In the evaluation of the MOMS-02/D2 triangulation accuracy, attention was focussed on the impact upon the bundle adjustment results of three variables: the number of control points and their distribution, the number of OIs, and the order of the Lagrange interpolation functions. Of the many triangulation adjustments conducted only a sample are considered here. The results presented have been obtained with the two independently observed sets of image coordinate data referred to earlier, namely a three-channel set from The University of Melbourne and a two-channel set from ETH Zurich. The former comprised a total of 62 points, the latter 48.

Tables 2 and 3 provide a summary of the accuracies obtained for the two data sets under conditions of differing numbers of control points and OIs, and changing orders for the interpolation functions for exterior orientation parameters. Listed in the tables are the RMS values of *XYZ* object coordinate discrepancies for the triangulated checkpoints for each bundle adjustment. In the cases of the 12 and 20 control points, the RMS discrepancy values listed are each effectively the means of the checkpoint residuals from two separate control point configurations (see Figure 1).

In comparing the results in Tables 2 and 3, the most striking feature is the fact that contrary to expectations (at least in planimetry) the 2-ray triangulation yields significantly superior accuracy to that of the 3-fold stereo imagery. This is thought to be partly a consequence of the superior quality of the image coordinates from ETH Zurich, which were measured with the aid of a more refined image enhancement process involving Wallis filtering and interactive quality evaluation. As has already been mentioned, there was a difference of 0.7 pixel (RMS) between the image coordinates of the two sets. This would account for a component of the discrepancy between the values listed in the two tables, which is generally at the level of 2-4m or up to 0.3 pixel for the LR channels.

Kornus et al (1995) refer to the appearance of unforeseen and unknown systematic effects in the MOMS-02/D2 image data which they attribute to calibration errors due possibly to in-flight changes in camera geometry. The presence of such systematic error in interior orientation is further indicated by the fact that the bundle adjustments of the three-fold stereo imagery yield poorer planimetric accuracy than the individual 2-D transformations for each channel. In spite of this, RMS point positioning accuracies at the 0.5 to 0.8 pixel level (with respect to the LR channels) are obtained.

A further quality measure of the ground point determination results is provided by a comparison of the internal precision (standard errors) and external accuracy (checkpoint discrepancies). Over the range of bundle adjustments of the 2-ray imagery represented in Table 2, the mean standard errors obtained from each of the covariance matrices C_x varied by only a modest amount and averaged $\sigma_{XY} \cong 4m$ and $\sigma_Z \cong 7m$. For the 3-ray triangulations of Table 3 the corresponding values were $\sigma_{XY} \cong 4m$ and $\sigma_Z \cong 10m$. The difference in heighting precision arises primarily as a consequence of the higher level of triangulation misclosure in the case of three-fold stereo coverage. Here, the RMS value of image coordinate residuals was close to 0.3 pixel, as compared to 0.2 pixel for the 2-ray triangulations. This influence of the difference in image coordinate residuals is balanced for planimetric precision by the stronger 3-ray intersection geometry.

Table 2: RMS values of checkpoint residuals in planimetry (S_{XY}) and height (S_Z) for adjustments of forward- and backward-looking channels only (image mensuration at ETH Zurich) for three control (Cl) point configurations. Units are metres.

Number of OIs	Order of Lagrange polynomial		Cl Pts. 4	Ck Pts. 44	Cl Pts. 12	Ck Pts. 36	Cl Pts. 20	Ck Pts. 28
	Position	Attitude	S_{XY}	S_Z	S_{XY}	S_Z	S_{XY}	S_Z
8	1	1	9.2	9.5	7.1	10.7	7.4	10.8
	2	2	8.8	5.2	6.6	6.3	6.8	7.1
	3	3	8.9	4.9	6.6	5.8	6.8	7.0
	3	1	8.7	4.6	7.2	6.3	6.9	6.9
6	1	1	13.1	9.0	9.7	14.0	9.8	15.0
	2	2	10.6	5.6	7.7	8.1	8.2	7.9
	3	3	10.6	5.7	7.7	5.1	6.3	6.7
	3	1	9.2	4.9	7.4	6.5	7.1	7.0

Table 3: RMS values of checkpoint residuals in planimetry (S_{XY}) and height (S_Z) for triangulation adjustments of 3-fold stereo imagery (image mensuration Melbourne University) for three control (Cl) point configurations. Units are metres.

Number of OIs	Order of Lagrange polynomial		Cl Pts. 4	Ck Pts. 58	Cl Pts. 12	Ck Pts. 50	Cl Pts. 20	Ck Pts. 42
	Position	Attitude	S_{XY}	S_Z	S_{XY}	S_Z	S_{XY}	S_Z
8	1	1	12.5	12.1	11.6	13.0	11.3	13.1
	2	2	10.8	8.8	10.7	9.9	11.1	11.0
	3	3	12.3	8.3	11.2	9.9	11.2	11.0
	3	1	11.2	7.4	11.4	8.0	11.3	10.0
6	1	1	15.4	12.2	13.9	14.8	12.9	13.3
	2	2	10.6	9.4	10.2	9.8	10.5	10.4
	3	3	10.5	9.2	10.1	9.8	10.5	10.2
	3	1	9.9	9.2	10.0	9.7	10.4	10.3

From Tables 2 and 3 it can be seen that there is reasonable agreement between the measures of precision and external accuracy for height determination, at least in the cases of 12 or more control points and second- or third-order Lagrange polynomials. In planimetry, however, the checkpoint discrepancy values are larger than the corresponding standard errors by a factor of at least 1.5. The corresponding factor for the three-fold stereo case is 2.5 or more. The cause of this difference can be largely attributed to the control point identification problem, and is likely also to be a consequence of uncompensated systematic error in the sensor system.

The apparent presence of residual systematic error, coupled with the control point identification problems, limited an in depth evaluation of the impact upon triangulation accuracy of control point distribution, number of OIs, and order of the Lagrange interpolation functions. The results listed in Tables 2 and 3 nevertheless provide some insight into these aspects.

5.2 Order of Lagrange Polynomials

Third-order Lagrange polynomials have found favour for the interpolation of position and attitude parameters for MOMS-02 (e.g. Ebner et al, 1992; Kornus et al, 1995). In the course of the present investigation it was decided to examine the impact of other orders for the polynomials. The 2-D transformation stage had indicated that second- and third-order functions might be most appropriate, yet analysis of the recovered attitude parameters suggested that their temporal variation was locally

linear. Moreover, there was initially some suspicion that bundle adjustments with a limited number of ground control points and third-order interpolation functions were subject to a measure of ill-conditioning which gave rise to possible projective compensation problems. This suspicion was reinforced by the results of a number of 'free-network' adjustments that were carried out (see Fraser & Shao, 1996).

The results listed in Tables 2 and 3 support the use of second- or third-order functions for the exterior orientation elements. It is noteworthy, however, that in the case of only four ground control points, the combination of third-order functions for positional parameters and a first-order model for attitude parameters yields the most accurate solution for both data sets, irrespective of the number of OIs.

5.3 Number of Orientation Images

The choice of the number of OIs is dependent upon a range of factors. These include the ability of the Lagrange polynomials of a given order to adequately model the temporal variations in position and attitude of the sensor over the distance between adjacent OIs. They also include consideration of the number and distribution of available ground control, which can impact upon the stability of the resulting normal equation system of the bundle adjustment. For this investigation, computations were performed with four, six and eight OIs, which corresponds approximately to an OI every 8000, 5300 and 4000 CCD lines, respectively. The time interval for the polynomial approximation in the case of eight OIs is about 8 sec.

As can be seen from Tables 2 and 3, there is little distinction between the results obtained for the cases of six and eight OIs, at least for adjustments incorporating polynomials of higher than first-order. This is also the case with changing the control point distribution, but here the two image data sets show different trends. In the 2-ray triangulation adjustment with 4 control points there is an increase in accuracy when adopting eight OIs instead of six. With the triangulation of the three-fold stereo imagery the opposite occurs, though in neither case are the changes significant.

Bundle adjustments with four OIs were also carried out. The triangulation accuracies obtained were significantly worse in height when first-order interpolation functions were employed, but were otherwise only marginally inferior, by 1-2m or so, to the corresponding accuracies for six and eight OIs.

5.4 Control Point Distribution

The five adopted ground control point configurations are indicated in Fig. 1. It should be recalled that the accuracies listed in Tables 2 and 3 represent the mean values obtained from adjustments for Sets 2 and 3 for the case of 12 control points, and for Sets 4 and 5 for the case of 20.

It is apparent from Table 2 that the number of control points has very little impact on the accuracy of ground point determination. It is hard to say whether this is a reflection of a strong 'relative orientation' of the three-fold stereo imagery or due to accuracy trends being concealed through the influence of residual systematic image errors coupled with control point identification problems. A similar masking of trends might well be at work in Table 3 where the results generally show an improvement in planimetric accuracy with the provision of additional control points. With heighting accuracy the situation is reversed, but again, the variations in accuracy are by no means significant.

6. CONCLUDING REMARKS

From the results obtained from triangulation of the imagery covering the Australian Testfield, it can be safely concluded that ground point determination to 10m (0.7 pixel) accuracy in planimetry and close to 6m (0.5 pixel) accuracy in height can be attained with MOMS-02. The drawing of further definitive conclusions regarding the influence of the difference in image mensuration quality between the HR and LR imagery, and in the control point distribution, number of orientation images and order of polynomial interpolation functions is unfortunately precluded due to both the quality of the ground point identification and the apparent presence of the unmodelled systematic errors alluded to by Kornus et al (1995).

7. REFERENCES

Ackermann, F., Bodechtel, J., Lanzl, F., Meissner, D., Seige, P. and Winkenbach, H., 1990. MOMS-02 - A multispectral stereo imager for the second German Spacelab Mission D2. *Int. Arch. Photogrammetry & Remote Sensing*, 28(1): 110-116.

Dorrer, E., Maier, W. and Uffenkamp, W., 1995. Analytical kinematic sensor orientation of MOMS-02 linear stereo imagery, *Proc. of Integrated Sensor Orientation: Theory, Algorithms, and Systems. Colomina/Navarro (eds.)*, Wichmann Verlag, pp. 261-273.

Ebner, H., Kornus, W. and Ohlhof, T., 1992. A simulation study on point determination for the MOMS-02/D2 space project using an extended functional model. *Int. Arch. Photogrammetry & Remote Sensing*, 29 (B4): 458-464.

Fraser. C.S. and Shao, J., 1996. On the triangulation accuracy of MOMS-02 three-line satellite imagery. *Geomatics Research Australasia*, No. 64 (in press).

Fraser, C.S., Fritsch, D., Collier, P.A. and Shao, J., 1996. Ground point determination using MOMS-02 Earth observation imagery. *Proc. 37th Australian Surveyors Congress*, Perth, 13-19 April, 19p.

Fritsch, D., 1994. Synergy of photogrammetry, remote sensing and GIS - the MOMS example. *Int. Arch. Photogrammetry & Remote Sensing*, 30(2): 2-9.

Kornus, W., Ebner, H. and Heipke, C., 1995. Photogrammetric point determination using MOMS-02/D2 imagery. *Proc. MOMS Symposium*, Cologne, Germany, July 5-7.

Kratky, V., 1989. Rigorous photogrammetric processing of SPOT images at CCM Canada. *ISPRS Journal of Photogrammetry and Remote Sensing*, 44: 53-71.

Seige, P., 1993. Status of the MOMS-02 experiment on the spacelab mission D2. *Proc. Int. Mapping from Space (ISPRS WG IV/2)*, Hannover, 15: 39-50.